Drug Delivery and Translational Research (2021) 11:984–999
https://doi.org/10.1007/s13346-020-00810-8

ORIGINAL ARTICLE

Topical instillation of triamcinolone acetonide-loaded emulsomes for posterior ocular delivery: statistical optimization and in vitro-in vivo studies

Rakhee Kapadia[1] · Kinjal Parikh[1] · Mahendra Jain[1] · Krutika Sawant[1]

Published online: 22 June 2020

Abstract

The objective of the present investigation was to formulate and characterize a novel lipid-based carrier-emulsomes loaded with triamcinolone acetonide (TA)/Nile red (NR) for non-invasive delivery to the posterior segment of the eye upon topical application. To optimize and delineate the effect of independent variables on dependent variables, Box-Behnken design (BBD) was adopted. The optimized batch was characterized for size, zeta potential, surface morphology by transmission electron microscopy, drug-excipient interaction by differential scanning calorimetry, osmolarity, pH, ex vivo transcorneal permeation, and stability studies. A short-term exposure (STE) test was performed on Statens Seruminstitut Rabbit Corneal (SIRC) cell lines to evaluate the in vitro ocular irritation. Precorneal retention study was performed in rabbit eyes. Confocal microscopy was used for ocular distribution studies in mice eye by preparing dye (Nile red)-loaded formulations. The surface response and contour plots along with ANOVA results demonstrated an interaction between the factors. The optimized batch had particle size of 131.17 ± 3.17 nm and entrapment efficiency of 71.56 ± 4.19%. TEM image showed unimodal, nano-sized emulsomes. TA-loaded emulsomes exhibited higher transcorneal permeation as compared to drug solution. In vitro irritation studies confirmed the safety of excipients for ophthalmic use. Fluorescence microscopic images obtained after ocular distribution studies showed strong fluorescence in inner and outer plexiform layers of the retina in comparison to dye solution confirming the delivery of dye to the posterior segment of mice eye after topical ocular instillation.

Keywords Emulsomes · Triamcinolone acetonide · Posterior ocular delivery · SIRC cell line · Topical instillation, HET-CAM

Introduction

After topical instillation, conventional formulations cannot reach the posterior segment of the eye because of various anatomical and physiological barriers along with the several precorneal factors which tend to remove the instilled drug. The longer diffusional distance—that the drug has to cross to reach the posterior segment of the eye—is an additional hurdle for the posterior ocular drug delivery [1–3]. Hence, particularly for the treatment of posterior ocular diseases, invasive methods (injections and surgical procedures) like direct injections into the periocular (subconjuctival, subtenon, retrobulbar) or vitreal region (intravitreal) of the eye are employed. In some cases, systemic (through oral or parenteral) routes are employed; however, through the former route, only 1–2% of drug reaches the ocular tissues while later needs administration by skilled person. Moreover, there are chances of side effects from the majority of dose remaining in the body [4].

Triamcinolone acetonide (TA), a synthetic glucocorticoid, possessing anti-inflammatory and anti-angiogenic properties is used to stop the progression of several inflammatory diseases of the posterior segment of the eye [5]. Generally, TA is administered by invasive methods such as subtenon, subconjunctival or intravitreal injections for posterior segment drug delivery, which leads to severe ocular complications. Furthermore, it is reported that TA has a short half-life in the vitreous fluid which in turn requires repeated intravitreal injection, ultimately leading to secondary complications such as postoperative infections, non-infectious endophthalmitis, and

Electronic supplementary material The online version of this article (https://doi.org/10.1007/s13346-020-00810-8) contains supplementary material, which is available to authorized users.

✉ Krutika Sawant
dr_krutikasawant@rediffmail.com

[1] Faculty of Pharmacy, The Maharaja Sayajirao University of Baroda, Kalabhavan, Vadodara, Gujarat 390 001, India

secondary ocular hypertension. There is also a hidden risk of infection, loss of vision, cataractogenesis, retinal bleeding, or retinal detachment. Moreover, subtenon and subconjunctival routes of administration also have shortcomings as the minimum therapeutic concentrations are not achieved because the drug could not penetrate enough into the vitreous fluid through these routes. This necessitates higher doses or multiple dosings of TA that possibly lead to increased intraocular pressure which might lead to the chain of other subsequent adverse effects [6]. Reviewing the complications of invasive therapy, it is understood that delivery of therapeutics to the posterior segment of eye demands novel non-invasive approach which decreases the complications and improves patient adherence [7].

Drug delivery to the posterior segments of the eye through topical instillation is of great clinical interest as it provides various advantages for direct and localized drug delivery to the target tissue, convenience, and relative painlessness [8]. However, conventional formulations such as eye drops, gels, and ointments are unable to achieve minimal therapeutic drug concentration in the retina owing to several anatomical and physiologic barriers such as tear film, cornea, and conjunctival barriers which limit the access of any exogenous substance/drug into the eye.

Strategic approaches that guarantee the long-term therapeutic effect with increased patient compliance are required for posterior drug delivery. Particularly, the use of nano-sized colloidal carriers can fulfill the need of noninvasive to a less invasive way of drug administration and can deliver the drug to the posterior segment of an eye either by corneal or by conjunctival/scleral route, or both, after topical administration [9]. Some researchers have previously explored the use of various colloidal carriers for posterior ocular delivery [10, 11]. Herein, we have proposed the use of novel lipid-based formulation, emulsomes, for non-invasive drug delivery to the posterior segment of the eye using the model drug—triamcinolone acetonide.

We have selected lipid-based nanocarriers as these materials are safe, non-toxic, non-irritant, and are body's natural component. Moreover, lipid carriers (1) can act as bionic tear film i.e., they mimic three-layered tear film of the eye and (2) they can enhance the residence in the eye by increasing the retention on conjunctival or corneal surfaces, or by enhancing the corneal penetration. Emulsomes are relatively unexplored new generation lipoidal vesicular system. It has an internal solid fat core surrounded by phospholipid bilayers. It is composed of a solidified or semi-solid internal core, usually made of triglycerides, diglycerides or monoglycerides, and one or more phospholipid layers stabilizing the internal core. It is in the form of an intermediate stage of liposome and o/w emulsion. It has been reported that this feature makes emulsomes more stable than liposomes. It is suitable for entrapment of both hydrophilic and hydrophobic drugs [12–14]. A monoglyceride, glyceryl monostearate (GMS), was selected as a solid lipid for the core of emulsomes; and the phospholipids, dipalmitoyl phosphatidylcholine (DPPC), and cholesterol were selected for bilayers of the emulsomes.

Henceforth, considering the problems associated with the invasive treatment and an issue pertaining to the TA molecule, in the present investigation, we formulated a non-invasive lipoidal nanocarrier that could deliver the drug to the posterior segment of eye after topical ocular instillation. The prepared emulsomes were optimized, characterized, and evaluated by several in vitro and in vivo methods for posterior ocular delivery after topical instillation.

Materials

TA was received as gift sample from Ranbaxy laboratories, Gurgaon, India. Dipalmitoyl phosphatidylcholine (DPPC) was received as a gift sample from Genzyme (Switzerland). Glyceryl monostearate (GMS), mannitol, and D (+) trehalose were purchased from Loba Chemie (Mumbai, India). Nile red (NR), Ultracel YM-100 filters, 3-(4,5-dimethylthiazol-2-yl)-2,5-diphenyltetrazolium bromide (MTT), and cholesterol were purchased from Sigma Aldrich (Mumbai, India). Chloroform (HPLC Grade) and methanol (HPLC grade) were purchased from Merck (Mumbai, India). Potassium dihydrogen phosphate, sodium hydroxide, sucrose, glycerol, and all other analytical reagents were obtained from SD Fine-Chem Limited (Vadodara, India). All other reagents used were of analytical grade. Cellulose dialysis tubing (molecular weight cut off 12,000), sterile PVDF membrane filter (pore size 0.22 μm and 0.45 μm), and 96-well plates were purchased from Himedia Lab (Mumbai, India). SIRC cell line was purchased from National Centre for Cell Sciences (NCCS, Pune, India). TearFlo™ Schirmer filter paper strips (2 mm × 7 mm) were purchased from Contacare Ophthalmics & Diagnostics (Gujarat, India). All other reagents were purchased from commercial sources and were of the highest available purity. Optimal cutting temperature compound (OCT compound) was purchased from Tissue-Tek® Sakura, USA.

Methods

Preparation and lyophilization of emulsomes

Various batches of TA-loaded emulsomes were prepared by thin-film hydration technique with slight modification as per laboratory set up [15]. In brief, TA (1.5 mg), DPPC, GMS (in different molar ratios), and cholesterol (0.2 mol of total lipids) were dissolved in 3 mL of chloroform in round-bottom flasks and were dried in a rotary evaporator under reduced pressure at 40 °C, to form thin lipid films. The films were dried in a

vacuum oven for 12 h to ensure complete removal of the solvent. Subsequently, the lipid films were hydrated by vortexing at 52 °C with distilled water (5 mL) to obtain TA-loaded emulsomes. The pH of the formulation was adjusted, if necessary, using 0.1 N NaOH to pH 6.8. Size of the resulting particles was then reduced by ultrasonication ((Labsonic® M, India) for the optimized time at 60% frequency to obtain desired particle size. The size of emulsomes was monitored and recorded at each stage of sonication by particle size Analyzer (Zeta sizer Nano series, Malvern Instruments, UK). Moreover, its effect on entrapment efficiency was also monitored.

The optimized TA-loaded emulsomes formulation was freeze-dried using lyophilizer (Heto Drywinner, Germany). Different cryoprotectants (Sucrose, Mannitol, and Trehalose dehydrate) in different ratios (1:3 w/w and 1:5 w/w) were screened to select the cryoprotectant which showed a minimum increment in particle size after reconstitution. Two ml of formulation with a respective concentration of cryoprotectant was frozen at − 70 °C for 6 h using deep freezer and finally lyophilized for 36 h under vacuum. Based on the results of the preliminary investigation, sucrose (1:3w/w) was selected as a cryoprotectant for lyophilization.

For ocular distribution studies, dye-loaded emulsomes were prepared by replacing the drug with Nile red (NR) dye. NR-loaded emulsomes were then separated from the free dye by centrifugation, and finally, these separated emulsomes were characterized for particle size and utilized immediately in experiments.

Estimation of TA

Estimation of TA was carried out as per the reported HPLC method with slight modifications [16].

HPLC condition Shimadzu LC-20 (Shimadzu, Kyoto, Japan) with a manual Rheodyne injector, 20-μL fixed loop and SPD-20A Prominence UV-Visible detector was used for estimation of TA. The separation was performed on a Vydac C18 column (particle size 5 μm, size 250*4.6 mm). Mobile phase contained a filtered and degassed mixture of acetonitrile, methanol, and water in the ratio of 30:60:10 (% v/v). The mobile phase was delivered at a flow rate of 1.5 mL/min and the injection volume was 20 μL. Run time was of 8 min. The analysis was performed at 254 nm. Chromatographic data were recorded and processed using Spinchrome Chromatographic Station CFR Version 2.4.0.193 (Spinchrome Pvt. Ltd., Chennai, India).

Entrapment efficiency (%EE)

The indirect method was adopted for the determination %EE of TA-loaded emulsomes. Free TA was separated from TA emulsomes by a filtration/centrifugation method and analyzed by the described HPLC method. In brief, prediluted samples with miliQ water were filtered by using centrifugal filter devices Ultracel YM-100 (Amicon® Millipore Corporation, Bedford, MA). Upon centrifugation at 3000 rpm for 15 min, the free drug was separated from the emulsomes (Sigma 301Kcentrifuge, Spain) which was quantified by above mentioned HPLC method. Furthermore, the entrapment efficiency was calculated by the following formula [17]:

$$\%\mathrm{EE} = \frac{\text{Total drug} - \text{Free drug}}{\text{Total drug added to emulsome formulation}} \times 100 \quad (1)$$

Optimization of emulsomes

Identification and risk assessment of critical quality attributes (CQA) for TA-loaded emulsomes

For ocular delivery of emulsomes, desired quality target product parameters were dosage form, dosage design, dosage strength, and drug product quality attributes such as particle size, %EE, assay, drug release, and stability. Risk analysis for the variables that might have effect on desired quality was carried out by a retrospective study. Initially, based on the literature survey, the risk factors having a significant effect on particle size and %EE (dependent variable) were identified [18]. Furthermore, risk assessment was carried out to identify critical parameters—a small change in which can significantly affect the desired product quality [19]. In this study, the highly affecting variables identified were DPPC:GMS ratio, lipid:drug ratio, and sonication time. Hence, their effects on the quality attributes (size and %EE) were studied using Box-Behnken design for optimization of the emulsomes.

Box-Behnken design

Emulsomes were optimized by response surface methodology (RSM). Box-Behnken design (BBD) is a nearly rotatable three-level incomplete factorial design [20]. It was selected to optimize the formulation variables at three levels (low, medium, and high, encoded as − 1, 0, and + 1). Effect of independent variables, i.e., DPPC:GMS ratio (A), lipid:drug ratio (B), and sonication time (C) was studied on dependent variables, i.e., size (Y1) and %EE (Y2). The Design-Expert software (version 8.0.4, State-Ease Inc., Minneapolis, USA) was used to run BBD, and for ANOVA study along with drawing of 2D contour plots and 3D surface response plots. The optimized batch was selected based on the desirability criteria. Percent prediction error of the prepared batch was calculated to evaluate the reliability of the developed mathematical model. The % prediction error was calculated by the following formula:

$$\%\text{Prediction error} = \frac{\text{Actual value} - \text{predicted value}}{\text{Actual value}} \times 100 \quad (2)$$

The levels and codes of variables considered in this study are shown in Table 1.

Characterization of emulsomes

Particle size (PS) and zeta potential (ζ)

Mean PS and polydispersity index (PDI) of TA-loaded emulsomes and NR-loaded emulsomes were determined by using dynamic light scattering (DLS) method (Zetasizer Nano ZS, Malvern, UK). For DLS principle-based size analysis, Nano ZS90 equipped with 4.0 mW internal laser was used. All measurements were performed in triplicate on the undiluted sample at 25 °C, at a scattering angle of 90°, and the intensity-weighted mean diameter was obtained for each sample [21].

The ζ of TA and NR-loaded emulsomes was measured using a folded capillary cell. The measurement was carried out at 25 °C in triplicate using multimodal analysis strategy. Smoluchowski approximation was used for zeta potential value determination [22].

Transmission electron microscopy (TEM)

TEM analysis was performed for morphology imaging of emulsomes. A drop of emulsomes dispersion containing 0.01% of phosphotungstic acid was placed on a perforated carbon film coated on a copper grid. The copper grid was fixed into a sample holder, placed in the vacuum chamber of the TEM machine, and observed under low vacuum. The grid was examined using transmission electron microscope (model Tecnai 20, 200 KV, Phillips, Netherland) [18].

Differential scanning calorimetry (DSC)

The thermo-analytical technique, DSC, measures difference in the amount of heat required to increase the temperature of sample and reference as a function of temperature [23]. The instrument (DSC-60) was calibrated with indium under nitrogen purging to avoid any kind of oxidative degradation. Thermal behavior of drug, its physical mixture with the excipients and formulation, was studied. For this, around 5 mg sample of drug, lipid and lyophilized emulsomes, was sealed in an aluminum pan which was heated from 25 to 300 °C under inert nitrogen atmosphere at a scanning rate of 10 °C/min.

Osmolarity and pH measurement

A well tolerated formulation is an important requirement in the treatment of several chronic diseases where frequent topical ocular drug administration is needed. Therefore, pH and osmolarity measurement of a topical formulation are necessary [16, 24, 25]. The osmolarity of optimized formulation was measured by freezing point depression measurements on an osmometer (Advanced Instruments INC). Briefly, 200 μL of TA emulsomes were taken in a disposable tube and osmometer probe was inserted in it. The instrument immediately displayed the osmolarity value. The pH of the TA emulsomes was measured by a pH meter and the final pH was adjusted similar to the tear pH~6.8.

In vitro short time exposure test (STE)

As an alternative to Draize test, cell line-based cytotoxicity methods have been employed for evaluating ocular irritation because they are cost-effective, sensitive, and easy to perform and score. For evaluating the ocular irritation (corneal toxicity), Statens Seruminstitut Rabbit Corneal (SIRC) epithelial cell lines are widely used. A short-term exposure test (STE test), which is an easy and accurate cell-based cytotoxicity method that can be used for evaluating the eye irritation potential of raw materials in vitro in rabbit derived corneal cells (SIRC cells), has been developed by Takahashi et al. [26].

In STE study, SIRC cells (7×10^3/well) in 96-well plates were exposed to 200 μL of 0.05%, 0.5%, and 5% (w/v) of test chemical solutions (DPPC, GMS, and TA) prepared by dissolving them either in physiological saline or saline with 5% (w/v) DMSO (according to the solubility of excipients) for 5 min. Each concentration of excipients was screened in triplicate. After exposure, the cells were washed with phosphate-buffered saline, and 200 μL of MTT dye solution (0.5 mg

Table 1 Variables in Box-Behnken design for TA-loaded emulsomes

Independent variables	Units	Coded values			Response (Y1)	Response (Y2)
		−1	0	1		
DPPC:GMS ratio (A)	Weight ratio	0.5:1	1:1	1.5:1	Particle size (nm)	% Entrapment efficiency
Lipid:drug ratio (B)	Weight ratio	10:1	20:1	30:1		
Sonication time (C)	Minutes	3	6	9		

MTT/mL of medium) was added. After a 2-h reaction time, MTT-formazan crystals were solubilized using DMSO for 2 h, and the absorbance of the solution was measured at 570 nm with a plate reader (Biorad, Model 680 XR, Mumbai, India).

The % ratio of MTT formazan absorbance for each test substance to that for control represented cell viability [26]. Following formula was used for calculation:

$$\%\ \text{Cell Viability (\%CV)} = \frac{\text{Absorbance of Samples}}{\text{Absorbance of Control}} \text{x } 100 \qquad (3)$$

The control group cells were treated with PBS pH 7.4. The study was carried out in triplicate, and the mean for these independent tests was used in the final analysis.

For each test concentrations, scores of 0, 1, or 2 were given, based on the % cell viability of STE test. The scores obtained on the basis of cell viability of 0.05% and 5% concentration of test chemicals were then added together to get the rank classification for eye irritation (Table 2). Finally, on the basis of % cell viability, the test chemicals used was characterized either as irritant (%CV < 70) or non-irritant (%CV > 70).

In vitro cell viability assay

The inhibition of cell growth by the TA-loaded emulsomes was assessed by MTT assay. Similar to STE test, SIRC cells were seeded in 96-well plate and left for seeding for 24 h prior to test. After completion of 24 h, the old media was discarded, and cells were incubated with various concentrations of TA-loaded emulsomes. The cells were also treated with Triton-X100 which acted as positive control and PBS pH 7.4 as negative control.

HET-CAM test

White fertile eggs obtained from hatchery were incubated for 9 days in fan-assisted egg incubator at 37 °C. On the last day, the eggs were torched from distance to ensure fertility. Non-viable or defective eggs were not used further. The test compound and controls were prepared such that, the final concentration of TA was 250 μg/mL. After 5 min of application of test material, any signs of lysis, hemorrhage, and coagulation were noted and compared with controls: 0.9% saline (negative control) and 0.1 M sodium hydroxide (positive control). Photographs were taken, and based on the severity of any hemorrhage, the test samples were graded on a scale from 0 (no reaction) to 3 (strong reaction). Scoring scale for HET-CAM is given in Table 3.

Table 3 Effect and score of HET-CAM assay

Effect	Score	Description
No hemorrhage	0	Non-irritant
Just visible membrane decolorization	1	Mild irritant
Structures are covered partially by hemorrhage	2	Moderate irritant
Structures are covered completely by hemorrhage	3	Severe irritant

Stability studies

Stability studies were performed for the lyophilized TA-loaded emulsomes. The lyophilized samples were kept in sealed glass vials and stored at refrigerated conditions (5 ± 3 °C) and room temperature (25 ± 2 °C, 60 ± 5% RH) for 3-month duration [27]. As per the stability protocol, the samples were withdrawn and analyzed for physicochemical parameters such as PS and drug content.

Ex vivo transcorneal permeation study

For transcorneal permeation study of TA-loaded emulsomes, isolated goat cornea model was used [28]. Freshly excised eyeballs were obtained from a slaughterhouse. The cornea was excised along with 2–4 mm of scleral tissue and washed with cold normal saline to remove the adhering tissue and proteins. Permeability study was performed using a diffusion cell. The receptor compartment comprised of 11 mL of PBS pH 7.4 maintained at 37.5 ± 2 °C on the thermostatic magnetic stirrer. Aliquot of formulation (equivalent to 87.5 μg drug) was placed over the cornea; samples were withdrawn every hour and analyzed for drug content by the validated HPLC method.

Table 2 Table for STE irritation score and STE rank after STE test

STE irritation score				STE rank = (0.05% score + 5% score)	Rank description
0.05% test concentration	Score	5% test concentration	Score	1	Minimally irritant
%CV > 70%	1	%CV > 70%	0	2	Moderate irritant
%CV ≤ 70%	2	%CV ≤ 70%	1	3	Severe irritant

% CV cell viability

The apparent permeation coefficient (Papp, cm/s) of TA was determined by the following formula:

$$\text{Papp}, Q = \frac{\Delta Q}{\Delta t} X \frac{1}{AC_{D0}} X \frac{1}{60} X\ 10,000,00 \quad (4)$$

where, C_{D0} is the initial concentration of drug in the donor compartment, and A is the area of the cornea. For the calculation of the apparent permeation coefficient in the present study, A was determined as 0.941 ± 0.26 cm^2. $\Delta Q/\Delta t$ is the steady-state rate of drug permeation across the intact cornea and was obtained from the slope of the straight line relating corneal permeability vs time.

In vivo studies

The animal study protocols were approved by the Institutional Animal Ethics Committee (IAEC), Faculty of Pharmacy, The Maharaja Sayajirao University of Baroda, Vadodara, India in accordance with the guidelines released by Committee for the Purpose of Control and Supervision of Experiments on Animals (CPCSEA), Ministry of Fisheries, Animal Husbandry and Dairying Department, Government of India, New Delhi, India.

Precorneal retention time

The drug concentration in the precorneal area was determined to evaluate the precorneal retention of formulation compared to TA solution by the reported method of Li et al. [29]. For these, New Zealand albino rabbits (male, weighing 2.5–3.0 kg) were used. Six rabbits were randomly divided into 2 groups.

For the precorneal retention time study, 150 μL of optimized TA emulsomes (drug equivalent to 26.25 μg) and TA solution was instilled in the lower conjunctival sac of both the eyes of rabbits. At pre-determined time intervals (5 min, 10 min, 30 min, 1 h, 2 h, 3 h, 4 h, 5 h, and 6 h), Schirmer paper strips (2 × 7 mm) were gently inserted into the lower eyelids of rabbits, and the eyes were closed to allow contact of the strip with ocular fluid for 30 s. After removal of the strip, to extract the drug, the strips were dipped in 1 mL of methanol and sonicated for 5 min in a bath sonicator (Ultrasonics Selec, Vetra, Italy) followed by vortexing for 5 min. The extracted drug solution was filtered using 0.22-μ membrane filter and analyzed by HPLC method. The pharmacokinetic parameters were calculated using Kinetica 5.0 pharmacokinetic data analysis software (Thermo ScientificTM, Thermofisher.com).

Ocular distribution studies

For the ocular distribution, a comparative study was carried out to identify the delivery efficiency of emulsomes [30]. For the same, a hydrophobic fluorescence probe Nile red (NR) incorporated into emulsomes and its molecular form (solution) were topically instilled in mice (female adult CD1 mice weighing 30–35 g). A single dose of 4 μL Nile red-loaded emulsomes or Nile red solution was instilled to the left eye. By the end of 30, 60, and 120 min after administration of the formulations ($n = 3$), both eyes were enucleated and gently irrigated with PBS. The specimen was fixed using 4% p-formaldehyde to preserve the morphological characteristics. Then, the specimen was immersed in 15% sucrose and 30% sucrose post-fix solution. The eyes specimen was then put in the embedding media (OCT compound) and rapidly frozen at − 25 °C, and sliced with a cryostat (Leica CM3050S, India) into 7-μm thick sections. The tissue sections were then placed onto slides and mounted with glycerol. The slides were observed using confocal microscopy (Carl Zeiss, Germany) in the wavelength of 550–700 nm. The "blank" was recorded from untreated tissue. The images were processed using ZEN imaging software [31].

Results and discussion

Topical application is the most desirable route for ocular drug delivery, even when the target tissues lie in the posterior segment, as severe side effects are associated with current treatment strategies (intraocular and systemic administration). Colloidal nano carriers are preferred for delivering drugs to posterior segment through topical route, as they can improve the drug bioavailability by multiple mechanisms such as increased surface area owing to their nano size and prolongation of pre-corneal retention time. The ideal colloidal formulation should have nano-size (ideally < 200 nm) and narrow size distribution ensuring low irritation and higher surface area to ocular tissues along with higher drug entrapment efficiency as these are the parameters that usually define the overall performance of the nano-formulation. Moreover, these parameters should not change upon long-term storage at a pre-defined condition, otherwise, the product performance in vivo would get affected. Hence, a preliminary investigation was done for critical factors to obtain a suitable working range and each factor was optimized using Box-Behnken design.

Optimization of emulsomes

Identification and risk assessment of critical quality attributes (CQA)

Various critical variables were identified after retrospective literature search which might have a significant effect on desired quality attributes, i.e., PS and %EE of emulsomes. From the multiple variables, few highly affecting variables were selected for primary investigation. Among the variables selected for primary investigation, DPPC:GMS ratio (internal lipid ratio), lipid:drug ratio, and sonication time were found

to be highly critical; hence these factors were selected to determine the design space using BBD.

Box-Behnken design

RSM was used to study the quantitative aspects of the effects and relationships among various formulation variables of emulsomes. BBD with a total of 17 experimental runs was selected to optimize the formulation parameters at three levels (Table 4).

Effect on dependent variables—PS and %EE

Effect of selected factors on PS was visible from the variation in PS obtained at different ratios of individual factor and combination of factors. The PS varied from 110.74 ± 7.01 to 141.01 ± 2.98 nm (Table 4).

The equation obtained for PS is summarized below:

$$Y_1 = 134.40 + 5.12A + 8.43B - 5.51C - 0.15AB + 1.85\,AC + 4.02\,BC - 6.25A^2 - 3.65B^2 + 0.15C^2 \ldots\ldots. \quad (5)$$

The result of ANOVA for the second-order quadratic equation for PS is given in Table 5. The goodness of the model can be checked by the determination of R^2. The value of adjusted R^2 (0.9988) suggests that the total variation of 99.88% for PS is attributed to the independent variables.

Table 4 Box-Behnken design matrix of TA-loaded emulsomes

Sr no.	DPPC:GMS ratio, A	Lipid: Drug ratio, B	Sonication time (s), C	Particle size (nm), Y1	%Entrapment efficiency, Y2
1	0	1	− 1	141.01 ± 2.98	80.17 ± 3.47
2	− 1	1	0	127.66 ± 4.32	67.10 ± 4.66
3	− 1	0	− 1	129.65 ± 4.98	69.52 ± 4.01
4	− 1	0	1	116.05 ± 6.55	57.91 ± 3.98
5	0	− 1	1	112.74 ± 6.34	56.83 ± 5.54
6	0	0	0	134.14 ± 3.98	72.92 ± 5.01
7	1	− 1	0	121.64 ± 5.76	60.81 ± 6.12
8	0	0	0	134.54 ± 3.76	72.82 ± 4.89
9	0	− 1	− 1	131.93 ± 3.65	68.80 ± 2.89
10	0	0	0	134.44 ± 4.12	72.51 ± 4.34
11	1	0	1	129.64 ± 2.47	64.22 ± 3.12
12	0	0	0	134.14 ± 3.12	72.54 ± 3.98
13	1	1	0	137.95 ± 3.54	75.91 ± 5.00
14	0	1	1	136.39 ± 2.19	68.70 ± 5.12
15	0	0	0	134.74 ± 4.43	72.91 ± 4.12
16	1	0	− 1	136.85 ± 3.22	76.92 ± 4.89
17	− 1	− 1	0	110.74 ± 7.01	58.11 ± 6.12

The effect of selected variables on PS can be visualized using 3D surface plots (Fig. 1a–c) and 2D contour plots (Fig. 1d–f).

From the Fig. 1, it is evident that while moving from − 1 to 0.5 level of factor A (DPPC:GMS ratio), PS increased, and on further moving from 0.5 to 1 level, it decreased. Factor B (lipid:drug ratio) had a positive effect on PS which means that with an increase in the value of B, increase in PS will be observed. Factor C (sonication time) demonstrated a negative effect on PS which means an increase in the value of factor C will lead to decrease in PS.

The effect of selected factors on %EE was visible at different ratios of individual factor and a combination of factors. The %EE varied from 58.11 ± 6.12 to 80.17 ± 3.47% (Table 4).

The equation obtained for %EE is summarized below:

$$Y_2 = 72.74 + 3.15\,A + 5.92B - 5.97C + 1.53AB - 0.27\,AC - 0.13\,BC - 4.37A^2 - 2.89B^2 - 1.23C^2. \quad (6)$$

The results of ANOVA of the second-order polynomial equation are given in Table 6 for %EE. Probability values (Prob > F) of less than 0.0500 in case of %EE showed that the model terms were significant. The p values of 0.0504 for %EE implied that the lack of fit was not significant relative to the pure error which was considered good. The value of adjusted R^2 (0.9972) suggests that the total variation of 99.72% in %EE is attributed to the independent variables, and only about 0.28% of the total variation cannot be explained by the model. For %EE, the predicted R^2 of 0.9836 was in reasonable agreement with the adjusted R^2 of 0.9972 between the experimental and predicted values of %EE [32].

Similar to PS, the effect of selected independent variables on %EE was also visualized using 3D surface plots and 2D contour plots (Fig. 2a–f).

Figure 2 indicates that factor A (DPPC:GMS ratio) has positive effect on %EE while moving from − 1 to 0.5 level, and thereafter from 0.5 to 1 level, it decreased which could be due to the formation of unstable vesicles at such a higher concentration of DPPC:GMS ratio. There was an overall increase in %EE while moving from − 1 to 1 level of factor B (lipid:drug ratio) while factor C (sonication time) has negative effect on %EE while moving from − 1 to 1 level.

Establishment of design space

The optimized batch was selected based on overall desirability factor calculated by Design-Expert software. The optimized formulation was carefully chosen by setting the criteria of maximum %EE and minimum PS. The calculated desirability factor was 0.628. The PS and %EE of the optimized batch can be observed in Table 7.

Table 5 ANOVA for the response surface quadratic polynomial model for PS

Response Y1	Particle size (nm)					
ANOVA for response surface quadratic model						
Analysis of variance table [partial sum of squares–type III]						
Source	Sum of Squares	Df	Mean Square	*F* Value	*p* value Prob > F	
Model	1332.63	9	148.0706	1536.62	< 0.0001	Significant
A-DPPC:GMS ratio	209.920	1	209.920	2178.48	< 0.0001	
B-Lipid:drug ratio	569.025	1	569.025	5905.15	< 0.0001	
C-Sonication time	243.211	1	243.211	2523.97	< 0.0001	
AB	0.09302	1	0.09302	0.96538	0.3586	
AC	13.6530	1	13.6530	141.686	< 0.0001	
BC	64.6416	1	64.6416	670.829	< 0.0001	
A^2	164.473	1	164.473	1706.85	< 0.0001	
B^2	56.1716	1	56.1716	582.930	< 0.0001	
C^2	0.09160	1	0.09160	0.95064	0.3620	
Residual	0.67452	7	0.09636			
Lack of fit	0.40252	3	0.13417	1.97316	0.2602	Not significant
Pure error	0.272	4	0.068			
Cor total	1333.30	16				

Characterization of emulsomes

Particle size, zeta potential, and entrapment efficiency

It was evident from the optimization study trials that the selected factors had a significant effect on the PS and %EE. Average PS of various batches of emulsomes was in the range of 110.74 ± 7.01 to 141.01 ± 2.98 nm. Optimized batch had mean PS of 131.17 ± 3.17 nm and polydispersity index (PDI) of 0.198 ± 0.021 indicating narrow size distribution. For ocular distribution studies, Nile red-loaded emulsomes were prepared, and their average PS was found to be 125.61 ± 3.19 nm,

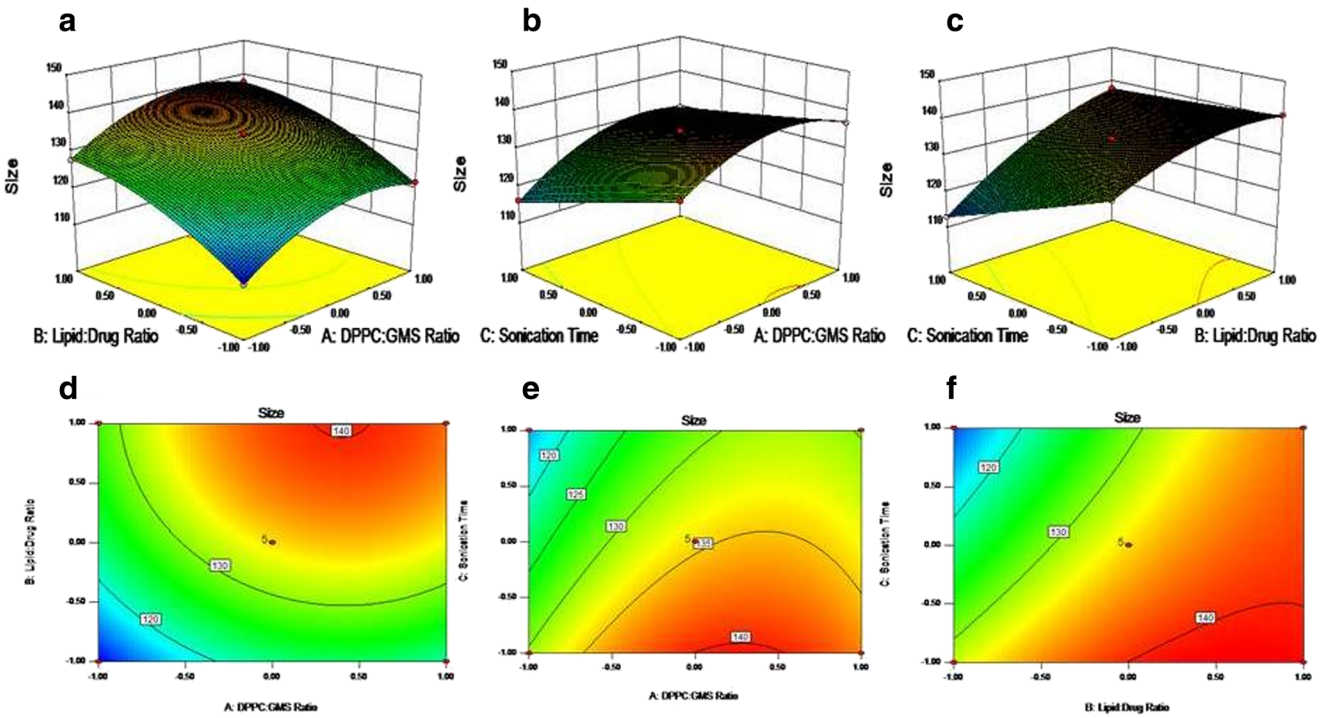

Fig. 1 Response surface plots and contour plots for particle size

Table 6 ANOVA for the response surface quadratic polynomial model for %EE

Response Y2	%Entrapment efficiency					
ANOVA for response surface quadratic model						
Analysis of variance table [Partial sum of squares–type III]						
Source	Sum of Squares	df	Mean Square	*F* Value	*p* value Prob > F	
Model	786.9278	9	87.43643	643.9126	< 0.0001	Significant
A-DPPC:GMS ratio	79.50605	1	79.50605	585.5105	< 0.0001	
B-Lipid:drug ratio	280.0161	1	280.0161	2062.137	< 0.0001	
C-Sonication time	285.0078	1	285.0078	2098.898	< 0.0001	
AB	9.333025	1	9.333025	68.73167	< 0.0001	
AC	0.297025	1	0.297025	2.187396	0.1827	
BC	0.0625	1	0.0625	0.460272	0.5193	
A^2	80.408	1	80.408	592.1528	< 0.0001	
B^2	35.10592	1	35.10592	258.5323	< 0.0001	
C^2	6.344237	1	6.344237	46.72119	0.0002	
Residual	0.950525	7	0.135789			
Lack of fit	0.789925	3	0.263308	6.558115	0.0504	Not significant
Pure error	0.1606	4	0.04015			
Cor total	787.8784	16				

which was almost near to TA-loaded emulsomes (131.17 ± 3.17 nm), indicating that the dye-loaded formulations could be used in place of drug-loaded emulsomes for ocular distribution studies in mice eye.

The various emulsome formulations showed zeta potential in the range of − 20 ± 2.85 to − 30 ± 2.13 mV. The observed negative charge on emulsomes could be attributable to the DPPC lipid. Optimized batch had zeta potential value of − 24.2 ± 2.12 mV. %EE of the prepared batches was in the range of 58.11 ± 6.12 to 80.17 ± 3.47%. Optimized batch had %EE of 71.56 ± 4.19%.

Transmission electron microscopy (TEM)

TEM image of TA emulsomes is shown in Fig. 3 which reveals discrete, nearly spherical unimodal emulsomes. The mean diameters of emulsomes were in the range of 100–

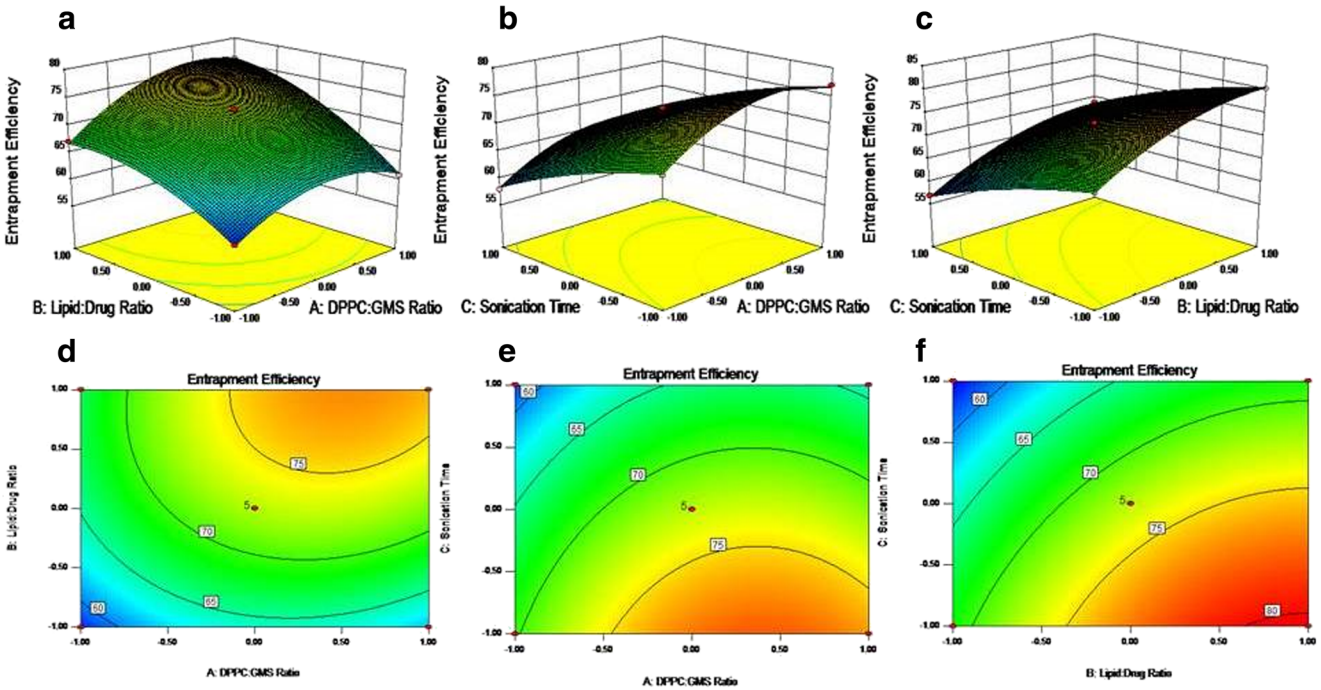

Fig. 2 Response surface plots and contour plots for entrapment efficiency

Table 7 Observed and predicted response variables of TA emulsomes

Variables–value	PS (nm)	%EE
A: DPPC:GMS ratio–0.75:1	Predicted–128.338 ± 4.19	Predicted–68.868 ± 3.95
B: Lipid:drug ratio–11.57:15.43	Actual–131.17 ± 3.17	Actual–71.56 ± 4.19
C: Sonication time–6	% Predicted error–2.98	% Predicted error–2.45

200 nm, which is in accordance with the results obtained from PS analysis by dynamic light scattering.

Differential scanning calorimetry (DSC)

DSC was performed on DPPC, GMS, TA, and lyophilized TA-loaded emulsomes. Since the melting point of TA was recorded at approximately 293 °C, DSC analysis was carried out from 25 to 300 °C. Figure 4a shows the DSC thermogram of (a) DPPC at 42.50 °C corresponding to its glass transition temperature, (b) GMS at 63.70 °C, and (c) pure TA at 290.09 °C indicating the crystalline anhydrous state of TA. While thermogram of lyophilized TA-loaded emulsomes showed only one peak at 41.20 °C indicating minor shifts in peak positions of DPPC, absence of characteristic melting endothermic peak of TA in lyophilized emulsomes indicates that TA is present in amorphous form and is molecularly dispersed in lipid matrix of emulsomes.

Osmolarity and pH measurement

For topical eye-drop formulation, osmolarity and pH are the most important factors. The osmolarity of a topically applied formulation often interferes with the ocular surface. Given that tears and eye drops are rapidly cleared in vivo from the eye surface, it is difficult to predict the actual level at which osmolarity might cause toxic effects. Ideally, osmolarity should be 300 mOsm/L. Clinically, a 6 times daily application of 380 mOsm/L formulation did not result in ocular surface alteration [33]. An in vitro study indicated that cultured corneal epithelium cells can tolerate upto 350 mOsm/L before cytotoxic effects occur [34].

Mean osmolarity of TA emulsomes was found to be 341 ± 2.32 mOsmol. Considering non-toxicity of 380 mOsm/L formulations, it can be assumed that osmolarity of 341 ± 2.32 mOsmol of the TA-loaded emulsomes will not develop any complications when used clinically.

The initial pH of the formulation was found to be 6.35 ± 1.41 which was then further adjusted with 0.05 M sodium hydroxide solution near to the tear pH~6.8.

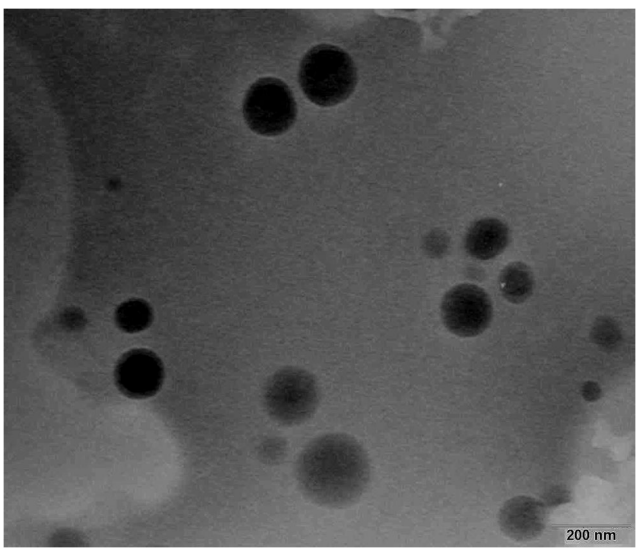

Fig. 3 TEM image of TA loaded emulsomes

In vitro short-term exposure test

Results showed that the excipients (DPPC and GMS) used in emulsomes formulation had viability above 70% at both 0.05 and 5% (w/v) concentrations (Fig. 4b). It gave them score 1 for 0.05% (w/v) concentration and score 0 for 5% (w/v) concentration. Now, according to the rank classification for ocular irritation, these two scores were added (score 1 (0.05%) + score 0 (5%) = rank 1) which gave them rank 1, which corresponds to chemicals being categorized as a minimal ocular irritant according to STE test. This indicated that the excipients chosen for the preparation of emulsomes, in the concentration range 0.05%, 0.5, and 5% (w/w), were minimal irritant and non-toxic to SIRC cell line, following 5-min exposure time.

In contrast, when cells were treated with free TA at equivalent concentration, 87.78 ± 2.31% cell viability was observed at 0.05% concentration which gave it a score 1 (%CV > 70%), and 69.12 ± 3.18% was observed at 5% (w/v) concentrations which gave it a score 1 (%CV ≤ 70%). For obtaining the rank classification, these two scores were added (score 1 (0.05%) + score 1 (5%) = rank 2) which gave it rank 2, that corresponds to chemicals being categorized as moderately ocular irritant. The observed decrease in cell viability at 5% w/v could be because of the aggregated or crystalline nature of TA at higher concentration [35, 36].

Earlier experimental and clinical work on TA (Kenacort-A®) showed that the product was toxic to lens and retina (retinal pigmented epithelial cells) because of the presence of benzyl alcohol, as the vehicle. Moreover, there were concerns about cytotoxicity caused by the crystalline form of aggregated

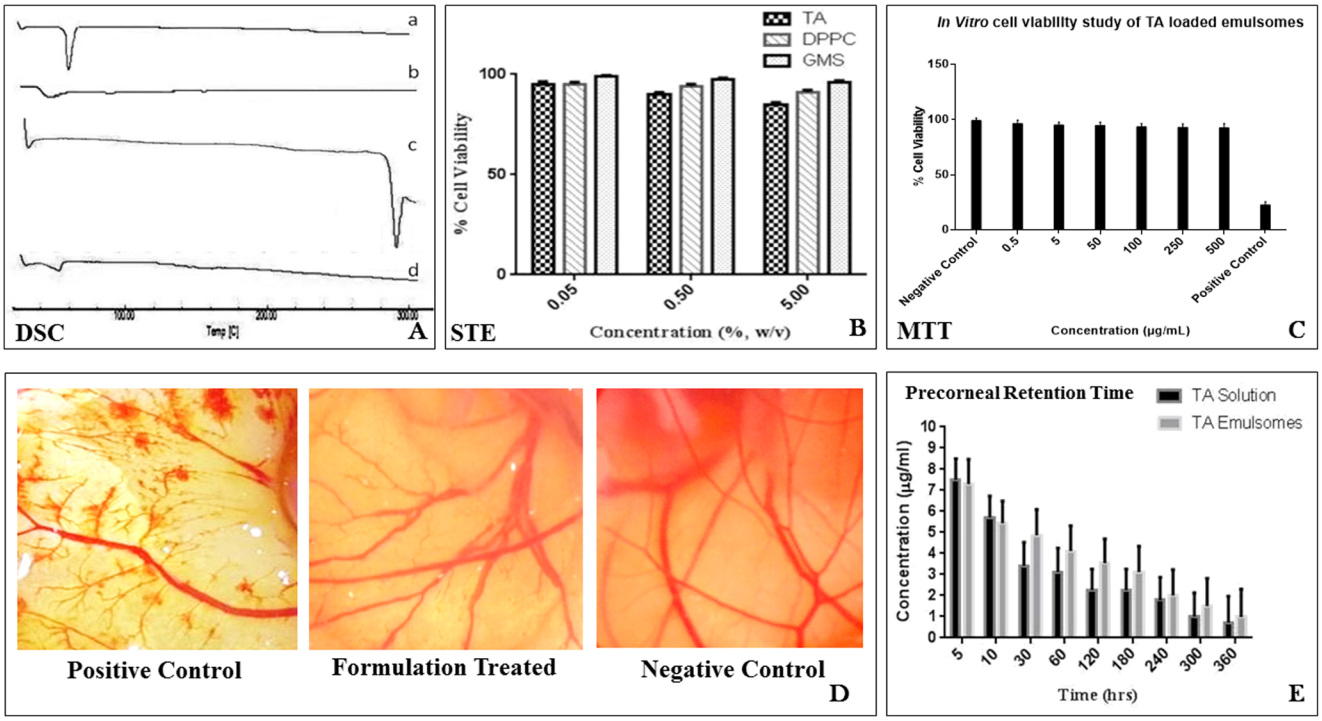

Fig. 4 **a** DSC thermogram of (a) DPPC, (b) GMS, (c) TA and (d) lyophilized TA emulsomes. **b** % cell viability of excipients used in TA emulsomes preparation at 0.05, 0.5, and 5% (w/v) concentration for STE study; each value represents the mean ± SD ($n = 3$). **c** % cell viability of TA-loaded emulsomes for MTT study, each value represents the mean ± SD ($n = 3$). **d** HET–CAM test. **e** Ocular tear concentration of TA from solution and emulsomes after topical administration in rabbit eye, each value represents the mean ± SD ($n = 3$)

TA, as well [35, 36]. Whereas, the results of STE indicate that the excipients used for the formulation development of TA-loaded emulsomes development would not be toxic.

In vitro cell viability assay

In the cell viability study through MTT assay, SIRC cells were incubated with a range of concentrations (0.5 to 500 μg/mL) of TA-loaded emulsomes for 24 h (Fig. 4c). Up to 70% reduction in the percent viability was observed for cells incubated with 100 μg/mL of Triton-X 100 (positive control). The percent cell viability data for SIRC cells was found to be > 80% for TA-loaded emulsomes, at all the studied concentrations. The cell viability at minimum incubation concentration of 0.5 μg/mL for TA-loaded emulsomes after 24 h was 96.6 ± 3.2%, showing non-significant decrease from the control value (p value = 0.3010), whereas at maximum concentration of 500 μg/mL also, 92.6 ± 3.9% cell viability was observed after 24 h (p value = 0.0624, compared with control). These results indicate that the prepared formulation studied in various concentration ranges on SIRC cells for a period of 24 h was non-toxic and safe.

HET-CAM test

The STE test simulates corneal toxicity; however, vascular effects such as the ones in the conjunctiva cannot be understood by STE. Hence, to evaluate acute toxicity of the prepared emulsomes formulation, Hen's Egg Test on Chorio Allantoic Membrane (HET-CAM) was performed. It allows to study immediate effects of test substance administration on the membrane of embryonated hen's egg. For ophthalmic irritancy, it is an established method and has shown good correlation to ophthalmic irritation with the in vivo situation. The membrane separates the embryo from the internal airspace, and is non-innervated, highly vascularized, and responds to injury in a similar way to rabbit conjunctiva [37].

The negative control, i.e., 0.9% saline produced no visual symptoms of irritation like hemorrhage or membrane discoloration after 5 min of application on the CAM. On the contrary, 0.1 M sodium hydroxide produced a severe hemorrhage giving it a score of 3, i.e., as a severe irritant. Whereas application of TA emulsomes on the CAM showed no signs of irritation or vascular response towards lysis, hence, it gave a score of zero, i.e., as non- irritant (Fig. 4d).

Stability studies

The data of stability studies of lyophilized TA emulsomes at 5 ± 3 °C and 25 ± 2 °C/60% ± 5% RH are shown in Table 8. It was observed that at both conditions, the lyophilized TA emulsomes were stable for up to 3 months. No significant change in either PS or drug content was observed, suggesting that the lyophilization of emulsomes in the presence of sucrose

Table 8 Stability profile of lyophilized TA-loaded emulsomes at 5 ± 3 °C and 25 ± 2 °C/60 ± 5%RH, each value represents mean ± SD ($n = 3$)

Sr no.	Time (months)	Particle size (nm)		Drug content (%)	
		2–8 °C	25–30 °C	2–8 °C	25–30 °C
1	0	143.81 ± 3.19	143.8 ± 3.19	99.16 ± 1.67	99.06 ± 1.67
2	1	144.00 ± 2.23	145.67 ± 3.01	99.03 ± 1.97	98.12 ± 3.18
3	2	147.01 ± 2.55	148.74 ± 2.95	98.65 ± 2.28	97.78 ± 2.95
4	3	150.45 ± 3.57	152.15 ± 3.07	98.15 ± 3.15	97.12 ± 3.14

maintained the size as well as assay of emulsomes at both storage conditions (5 ± 3 °C and at 25 ± 2 °C/60% ± 5% RH).

Ex vivo transcorneal permeation study

From the ex vivo corneal permeation of TA, Papp values were calculated. As compared to TA solution, higher corneal permeation was observed for TA emulsomes. The measured Papp value of TA solution was 2.39 ± 0.60 cm/s, which might be owing to its higher lipophilic nature. Moreover, the upper epithelial layers of the cornea are also hydrophobic in nature, hence TA might have displayed higher corneal permeability. The increased permeation from the emulsomes as compared to solution may be because of higher retention of nanoparticles on the corneal surface due to nano size of the particles.

The Papp of TA emulsomes was found to be 3.84 ± 0.82 cm/s, which is higher than the TA solution and could be related to the composition of emulsomes. The outer layer of emulsomes is composed of phospholipids that will come in intimate contact with the outer ocular barriers, such as cornea and conjunctiva. These lipidic components of the emulsomes will interact with the lipidic layer of the tear film, enabling the carriers to remain in the corneal and conjunctival sac for a long time and can facilitate corneal permeation thereby increasing the ocular bioavailability of drugs [38, 39]. This increased transcorneal permeability of emulsomes can also be correlated to those of liposomes, as the external structure of both lipoidal carriers is made up of phospholipids, and it is already reported that when applied topically, liposomes attach to the hydrophobic corneal epithelium, where it continuously releases the bound drug content, improving pharmacokinetics and decreasing toxic side effects [40, 41].

In vivo studies

Precorneal retention time

After in vivo instillation of TA emulsomes and TA solution into the conjunctival sac, the drug concentration was determined in rabbit lachrymal fluid. The graph of TA concentration (μg/mL) vs time is shown in Fig. 4e. For the first time point, the TA tear film concentration was high for TA solution and emulsomes both.

After 10 min, a decrease in concentration was observed, which was due to the mechanical elimination of excess instilled volume from the cul-de-sac, as lower eyelid cannot hold more than 50 μL volume, and administration of higher volume of formulation would ultimately lead to overflow of the drop from the eyes [42]. After 30 min, the concentration of TA decreased constantly for the TA solution. Whereas in the case of TA emulsomes, drug concentration was higher at each time point as compared to TA solution, which could be because of the prolonged retention of emulsomes in the precorneal area. Emulsomes provide an intimate contact between drug and ocular surface tissues, thus, facilitating the penetration of the drug into cornea, aqueous humor, and conjunctiva. Moreover, lipid vesicles also permeate through the ocular surface by several biological mechanisms such as fusion, adsorption, endocytosis, and lipid exchange [1]. Lipidic components of the emulsomes interact with the lipid layer of the tear film, enabling the nanocarrier to remain in the conjunctival sac for a long time, where they act as a drug depot and release drug for a longer period. Also, the phospholipids used in the formulation have been found to interact with the muco-aqueous layer and lipid layer and could have improved the "wettability" of tear film, thereby increasing the residence time of drugs on ocular surfaces [41, 43].

The area under the curve (AUC) for TA emulsomes was 17.3203 μg/mL*h, which was significantly higher than of TA solution (12.2558 μg/mL*h) (p value = 0.029). Tmax for both the TA emulsomes and solution was same, i.e., 5 min. Whereas, Cmax was higher for solution, i.e., 7.7 μg/mL, for TA emulsomes − 7.3 μg/mL. The difference in Cmax was owing to emulsomes' structure which sustained release of drug from the vesicles. These results indicate that as compared to the TA solution, TA emulsomes were retained for a longer time in the precorneal area, facilitating increased drug permeability and ultimately ocular bioavailability.

Ocular distribution studies

Confocal microscopy was used to study the intraocular distribution of NR-loaded emulsomes applied as eye drops in the mice eye. The inner plexiform layer (IPL) is reported as a suitable target for evaluating retinal delivery since it is located

very close to the ganglion cell layer (GCL), containing retinal ganglion cells and amacrine cells.

Figure 5a–e show the flat-mount images of different sections of an eye after administration. Figure 5a shows that very little fluorescence was visible in the case of eyes treated with Nile red solution. Figure 5b shows the corneal image of eyes after 30 min of topical administration of Nile red-loaded emulsomes. Corneal epithelium, corneal stroma, and endothelial layer are evident in the figure. Strong fluorescence was observed on the surface of the cornea and stroma suggesting that these nanocarriers might have accumulated on the surface of cornea and eventually followed the corneal route for delivery of small molecules into the posterior segment of the eye by virtue of their size and composition

Nano size of the carrier plays a crucial role in retinal drug delivery through transcorneal route as nano size of particles represents a greater surface area available for the association between the cornea and the conjunctiva [44]. Moreover, previous research on ocular drug delivery after topical instillation of different sized liposomes showed that size of around 100 nm provided the most effective delivery of a fluorescent probe to the mouse retina after topical administration [45]. Due to their small sizes, nano-drug carriers are likely to have high diffusivity across membranes such as the corneal epithelium. Similarly, due to their high surface area to volume ratio, nano-sized carriers also show improved interaction with the outer membrane of the corneal surface, thereby, prolonging the retention of the topically administered drug. Moreover, they effectively deliver the drug to intraocular tissues such as the retina by noninvasive delivery [46]. Penetration and distribution of drug-loaded emulsomes into the posterior tissues of the eye after topical administration seemed to occur mainly via three routes: the corneal, conjunctival, and systemic. (1) Drug can diffuse into the iris root and subsequently into the posterior chamber aqueous humor and into the posterior tissues. (2) Drug can diffuse across the sclera by lateral diffusion followed by penetration of Bruch's membrane and the retinal pigment epithelium (RPE). (3) To a lesser extent, the drug can be absorbed into the systemic circulation either through the conjunctival vessels or via nasolacrimal duct and gain systemic access to the retinal vessels [47].

In this study, NR-loaded emulsomes were prepared and the optimized batch had PS of 131.17 ± 3.17 nm, which suggests their suitability as an ophthalmic nanocarrier and could be one of the reasons for longer retention of these carriers on the surface of the cornea. Particle size is certainly a foremost parameter for effective retinal delivery. Other factor that plays an important role in retinal drug delivery is the composition of the nanocarriers. Lipid-based nanocarriers are particularly useful in topical ocular delivery as they act as "bionic tear film" which improves drug bioavailability by enhancing the residence time on the ocular surface and also by enhancing corneal penetration [41]. The transcorneal absorption, transfer of drug into corneal epithelial cell layer, and other mechanisms such as endocytosis or fusion of phospholipid bilayer membrane might have contributed to increased permeation of emulsomes as compared to the solution [48].

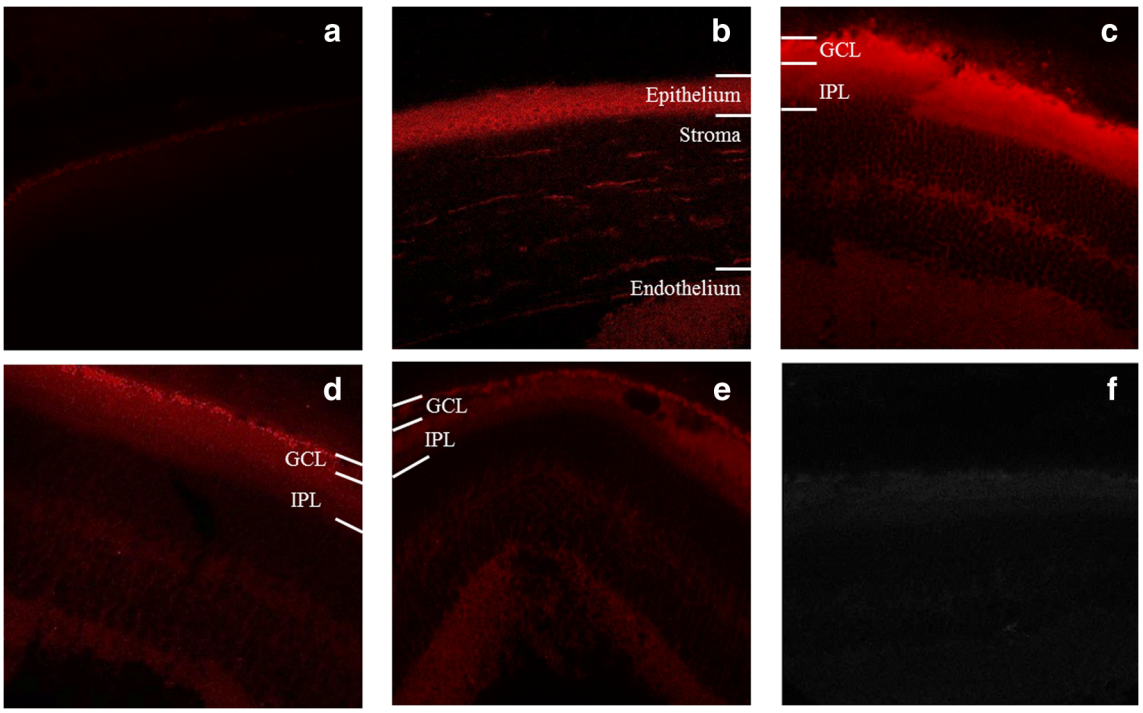

Fig. 5 Fluorescence microscopic images of **a** NR solution in retina after 30 min, **b** NR-loaded emulsomes in cornea after 10 min, **c** in retina after 30 min, **d** in retina after 60 min, and **e** in retina after 120 min. **f** Tissue imaged at the same wavelength as used for NR-loaded emulsomes

Figure 5c–e show the fluorescence microscopic images of NR loaded emulsomes in retina after 30, 60, and 120 min of topical application, respectively. Strong fluorescence can be observed clearly in the inner and outer plexiform layers (IPL and OPL layers) along with other layers of retina. The highest fluorescence was observed at around 30 min, which declined by 60 min and disappeared within 120 min which might be owing to the clearance of emulsomes or because of the episcleral or choroidal circulation which plays an important role in clearing drugs after subconjunctival application. The strong fluorescence in the IPL layer suggests that these NR-loaded emulsomes might have reached the posterior segment of the eye by either corneal or conjunctival pathways or both.

Figure 5f shows tissue imaged at the same wavelength as used for NR-loaded emulsomes. This was carried out to verify autofluorescence from various retinal layers. As there was not any fluorescence observed, it confirms that the fluorescence observed as in Fig. 5a–e was due to true NR labeling and not auto-fluorescence.

Although these initial studies of the prepared emulsomal formulation on mice eyes showed positive result for posterior ocular delivery after topical administration, several other factors should also be kept in mind such as the size and ocular barriers of the eye [49]. Therefore, further experiments in higher animals are needed to confirm the penetration of NR to the retina after topical administration.

Conclusions

Triamcinolone acetonide (TA), a glucocorticoid, is currently administered by intravitreal administration for the long-term management of various inflammatory ocular diseases. Due to its invasive administration techniques, it imposes a high risk of ocular damage. Hence, in the present research work, we have reported the development and evaluation of the lipid-based nano-sized carrier, emulsomes, as a novel vehicle for delivering TA to the posterior segment of eye after topical ocular instillation. Emulsomes of PS below 200 nm were successfully prepared by thin-film hydration method. The optimized batch selected by applying BBD had PS of 131.17 ± 3.17 nm and %EE of 70.56 ± 4.19%. As compared to conventional drug solution, results of both ex vivo corneal permeation study and in vivo precorneal retention study indicated higher transcorneal permeation and retention of TA from emulsomes. This could be attributable to the increased interaction and retention of lipid-based nanocarriers—emulsomes with the lipid layer of the tear film and corneal surface, which ultimately increases the ocular bioavailability of TA. Fluorescence microscopic images obtained after ocular distribution studies showed strong fluorescence in inner and outer plexiform layers of the retina in comparison to dye solution suggesting that the dye-loaded emulsomes reached the posterior segment of eye after topical ocular instillation. These initial investigations in animals indicate that the developed nano-sized emulsomes formulation can be used as an alternative to currently used invasive treatment strategies for the treatment of diseases of the posterior segment of the eye. This initial study in mice suggests that emulsomes can be a promising carrier for posterior ocular drug delivery after topical administration, and further detailed research on the use of these novel nanocarriers can open up new avenues for ocular drug delivery research.

Acknowledgments The authors duly acknowledge Ranbaxy laboratories, Gurgaon, India for providing Triamcinolone acetonide as gift sample and Genzyme (Switzerland) for gift sample of DPPC.

Funding information This study received financial assistance from Indian Council for Medical Research, New Delhi, India for providing Senior Research Fellowship to Rakhee Kapadia and TIFAC CORE in NDDS, DST, Government of India, New Delhi, India for providing the research facility.

Compliance with ethical standards

Conflict of interest The authors declare that they have no conflict of interest.

References

1. Lalu L, Tambe V, Pradhan D, Nayak K, Bagchi S, Maheshwari R, et al. Novel nanosystems for the treatment of ocular inflammation: current paradigms and future research directions. J Control Release. 2017;268:19–39. https://doi.org/10.1016/j.jconrel.2017.07.035.
2. Nayak K, Misra M. A review on recent drug delivery systems for posterior segment of eye. Biomed Pharmacother. 2018;107:1564–82. https://doi.org/10.1016/j.biopha.2018.08.138.
3. Pandhare A, Bhatt P, Saluja HS, Pathak YV. Biodegradable polymeric implants for retina and posterior segment disease. In: Patel JK, Sutariya V, Kanwar JR, Pathak YV, editors. Drug delivery for the retina and posterior segment disease. Cham: Springer International Publishing; 2018. p. 273–91.
4. Tekade RK, Tekade M. Ocular bioadhesives and their applications in ophthalmic drug delivery. In: Nano-Biomaterials For Ophthalmic Drug Delivery. Springer; 2016. p. 211–30.
5. Couch SM, Bakri SJ. Intravitreal triamcinolone for intraocular inflammation and associated macular edema. Clin Ophthalmol. 2009;3:41–7. https://doi.org/10.2147/opth.s4477.
6. Phulke S, Kaushik S, Kaur S, Pandav SS. Steroid-induced glaucoma: an avoidable irreversible blindness. J Curr Glaucoma Pract. 2017;11(2):67–72. https://doi.org/10.5005/jp-journals-l0028-1226.
7. Eljarrat-Binstock E, Pe'er J, Domb AJ. New techniques for drug delivery to the posterior eye segment. Pharm Res. 2010;27(4):530–43. https://doi.org/10.1007/s11095-009-0042-9.
8. Gaudana R, Ananthula HK, Parenky A, Mitra AK. Ocular drug delivery. AAPS J. 2010;12(3):348–60. https://doi.org/10.1208/s12248-010-9183-3.
9. Weng Y, Liu J, Jin S, Guo W, Liang X, Hu Z. Nanotechnology-based strategies for treatment of ocular disease. Acta Pharm Sin B. 2017;7(3):281–91. https://doi.org/10.1016/j.apsb.2016.09.001.
10. Gupta S, Dube A, Vyas SP. Antileishmanial efficacy of amphotericin B bearing emulsomes against experimental visceral

leishmaniasis. J Drug Target. 2007;15(6):437–44. https://doi.org/10.1080/10611860701453836.
11. Narvekar P, Bhatt P, Fnu G, Sutariya V. Axitinib-loaded poly(lactic-co-glycolic acid) nanoparticles for age-related macular degeneration: formulation development and in vitro characterization. Assay Drug Dev Technol. 2019;17(4):167–77. https://doi.org/10.1089/adt.2019.920.
12. Gandhi M, Pandya T, Gandhi R, Patel S, Mashru R, Misra A, et al. Inhalable liposomal dry powder of gemcitabine-HCl: formulation, in vitro characterization and in vivo studies. Int J Pharm. 2015;496(2):886–95. https://doi.org/10.1016/j.ijpharm.2015.10.020.
13. Gill B, Singh J, Sharma V, Kumar SLH. Emulsomes: an emerging vesicular drug delivery system. Asian J Pharm. 2014;6(2).
14. Paliwal R, Paliwal SR, Mishra N, Mehta A, Vyas SP. Engineered chylomicron mimicking carrier emulsome for lymph targeted oral delivery of methotrexate. Int J Pharm. 2009;380(1–2):181–8. https://doi.org/10.1016/j.ijpharm.2009.06.026.
15. Anselem S, Lowell GH, Aviv H, Friedman D. Solid fat nanoemulsions as vaccine delivery vehicles. Google Patents. 1998.
16. Araujo J, Nikolic S, Egea MA, Souto EB, Garcia ML. Nanostructured lipid carriers for triamcinolone acetonide delivery to the posterior segment of the eye. Colloids Surf B: Biointerfaces. 2011;88(1):150–7. https://doi.org/10.1016/j.colsurfb.2011.06.025.
17. Pandya NT, Jani P, Vanza J, Tandel H. Solid lipid nanoparticles as an efficient drug delivery system of olmesartan medoxomil for the treatment of hypertension. Colloids Surf B: Biointerfaces. 2018;165:37–44. https://doi.org/10.1016/j.colsurfb.2018.02.011.
18. Kamani P, Parikh K, Kapadia R, Sawant K. Phospholipid based ultra-deformable nanovesicular gel for transcutaneous application: QbD based optimization, characterization and pharmacodynamic profiling. J Drug Delivery Sci Technol. 2019;51:152–63. https://doi.org/10.1016/j.jddst.2019.02.035.
19. Parmar C, Parikh K, Mundada P, Bhavsar D, Sawant K. Formulation and optimization of enteric coated bilayer tablets of mesalamine by RSM: in vitro – in vivo investigations and roentogenographic study. J Drug Delivery Sci Technol. 2018;44:388–98. https://doi.org/10.1016/j.jddst.2018.01.008.
20. Javia A, Thakkar H. Intranasal delivery of tapentadol hydrochloride-loaded chitosan nanoparticles: formulation, characterisation and its in vivo evaluation. J Microencapsul. 2017;34(7):644–58. https://doi.org/10.1080/02652048.2017.1375038.
21. Parikh KJ, Sawant KK. Solubilization of vardenafil HCl in lipid-based formulations enhances its oral bioavailability in vivo: a comparative study using Tween - 20 and Cremophor - EL. J Mol Liq. 2019;277:189–99. https://doi.org/10.1016/j.molliq.2018.12.079.
22. Gandhi M, Bhatt P, Chauhan G, Gupta S, Misra A, Mashru R. IGF-II-conjugated nanocarrier for brain-targeted delivery of p11 gene for depression. AAPS PharmSciTech. 2019;20(2):50. https://doi.org/10.1208/s12249-018-1206-x.
23. Christian R, Thakkar V, Patel T, Gohel M, Baldaniya L, Shah P, et al. Development of biodegradable injectable in situ forming implants for sustained release of lornoxicam. Curr Drug Deliv. 2019;16(1):66–78. https://doi.org/10.2174/1567201815666180927155710.
24. Agrahari V, Mandal A, Agrahari V, Trinh HM, Joseph M, Ray A, et al. A comprehensive insight on ocular pharmacokinetics. Drug Deliv Transl Res. 2016;6(6):735–54. https://doi.org/10.1007/s13346-016-0339-2.
25. Alshamrani M, Sikder S, Coulibaly F, Mandal A, Pal D, Mitra AK. Self-assembling topical nanomicellar formulation to improve curcumin absorption across ocular tissues. AAPS PharmSciTech. 2019;20(7):254. https://doi.org/10.1208/s12249-019-1404-1.
26. Takahashi Y, Koike M, Honda H, Ito Y, Sakaguchi H, Suzuki H, et al. Development of the short time exposure (STE) test: an in vitro eye irritation test using SIRC cells. Toxicol in Vitro. 2008;22(3):760–70. https://doi.org/10.1016/j.tiv.2007.11.018.
27. Guideline, ICH Harmonised Tripartite, Stability Testing of new Drug Substances and Products. Q1A (R2). 2003.
28. Yadav M, Ahuja M. Preparation and evaluation of nanoparticles of gum cordia, an anionic polysaccharide for ophthalmic delivery. Carbohydr Polym. 2010;81(4):871–7. https://doi.org/10.1016/j.carbpol.2010.03.065.
29. Li N, Zhuang C, Wang M, Sun X, Nie S, Pan W. Liposome coated with low molecular weight chitosan and its potential use in ocular drug delivery. Int J Pharm. 2009;379(1):131–8. https://doi.org/10.1016/j.ijpharm.2009.06.020.
30. Araujo J, Vega E, Lopes C, Egea MA, Garcia ML, Souto EB. Effect of polymer viscosity on physicochemical properties and ocular tolerance of FB-loaded PLGA nanospheres. Colloids Surf B: Biointerfaces. 2009;72(1):48–56. https://doi.org/10.1016/j.colsurfb.2009.03.028.
31. Pandey A, Singh K, Patel S, Singh R, Patel K, Sawant K. Hyaluronic acid tethered pH-responsive alloy-drug nanoconjugates for multimodal therapy of glioblastoma: an intranasal route approach. Mater Sci Eng C. 2019;98:419–36. https://doi.org/10.1016/j.msec.2018.12.139.
32. Parikh KJ, Sawant KK. Comparative study for optimization of pharmaceutical self-emulsifying pre-concentrate by Design of Experiment and Artificial Neural Network. AAPS PharmSciTech. 2018;19(7):3311–21. https://doi.org/10.1208/s12249-018-1173-2.
33. Dutescu RM, Panfil C, Schrage N. Osmolarity of prevalent eye drops, side effects, and therapeutic approaches. Cornea. 2015;34(5):560–6.
34. Kang SS, Ha SJ, Kim ES, Shin JA, Kim JY, Tchah H. Effect of nerve growth factor on the in vitro induction of apoptosis of human conjunctival epithelial cells by hyperosmolar stress. Invest Ophthalmol Vis Sci. 2014;55(1):535–41. https://doi.org/10.1167/iovs.13-12459.
35. Narayanan R, Mungcal JK, Kenney MC, Seigel GM, Kuppermann BD. Toxicity of triamcinolone acetonide on retinal neurosensory and pigment epithelial cells. Invest Ophthalmol Vis Sci. 2006;47(2):722–8. https://doi.org/10.1167/iovs.05-0772.
36. Szurman P, Kaczmarek R, Spitzer MS, Jaissle GB, Decker P, Grisanti S, et al. Differential toxic effect of dissolved triamcinolone and its crystalline deposits on cultured human retinal pigment epithelium (ARPE19) cells. Exp Eye Res. 2006;83(3):584–92. https://doi.org/10.1016/j.exer.2006.02.012.
37. Luepke NP, Kemper FH. The HET-CAM test: an alternative to the draize eye test. Food Chem Toxicol. 1986;24(6):495–6. https://doi.org/10.1016/0278-6915(86)90099-2.
38. Mainardes RM, Urban MC, Cinto PO, Khalil NM, Chaud MV, Evangelista RC, et al. Colloidal carriers for ophthalmic drug delivery. Curr Drug Targets. 2005;6(3):363–71. https://doi.org/10.2174/1389450053765914.
39. Alany RG, Rades T, Nicoll J, Tucker IG, Davies NM. W/O microemulsions for ocular delivery: evaluation of ocular irritation and precorneal retention. J Control Release. 2006;111(1–2):145–52. https://doi.org/10.1016/j.jconrel.2005.11.020.
40. Chetoni P, Burgalassi S, Monti D, Najarro M, Boldrini E. Liposome-encapsulated mitomycin C for the reduction of corneal healing rate and ocular toxicity. J Drug Delivery Sci Technol. 2007;17(1):43–8. https://doi.org/10.1016/S1773-2247(07)50006-7.
41. Gan L, Wang J, Jiang M, Bartlett H, Ouyang D, Eperjesi F, et al. Recent advances in topical ophthalmic drug delivery with lipid-based nanocarriers. Drug Discov Today. 2013;18(5–6):290–7. https://doi.org/10.1016/j.drudis.2012.10.005.
42. Blazka M, Hayes W. Chapter 22: acute toxicity and eye irritancy. In: Hayes A, editor. Principles and methods of toxicology. Boca Raton: CRC Press; 2008. p. 1131–78.

43. Zabell M. Phospholipids: the glue that holds the tear film together? https://www.mieducation.com/pages/phospholipids-the-glue-that-holds-the-tear-film-together#:~:text=Inthecaseofthe,thetearfilmlipidlayer. Accessed 07/06/2020.
44. Diebold Y, Calonge M. Applications of nanoparticles in ophthalmology. Prog Retin Eye Res. 2010;29(6):596–609. https://doi.org/10.1016/j.preteyeres.2010.08.002.
45. Inokuchi Y, Hironaka K, Fujisawa T, Tozuka Y, Tsuruma K, Shimazawa M, et al. Physicochemical properties affecting retinal drug/Coumarin-6 delivery from nanocarrier systems via eyedrop administration. Invest Ophthalmol Vis Sci. 2010;51(6):3162–70. https://doi.org/10.1167/iovs.09-4697.
46. Liu S, Jones LW, Gu FX. Nanotechnology and nanomaterials in ophthalmic drug delivery. In: Pathak Y, Sutariya V, Hirani A, editors. Nano-Biomaterials For Ophthalmic Drug Delivery. Springer; 2016. p. 83–109.
47. Hughes PM, Olejnik O, Chang-Lin JE, Wilson CG. Topical and systemic drug delivery to the posterior segments. Adv Drug Deliv Rev. 2005;57(14):2010–32. https://doi.org/10.1016/j.addr.2005.09.004.
48. Amrite AC, Kompella UB. Size-dependent disposition of nanoparticles and microparticles following subconjunctival administration. J Pharm Pharmacol. 2005;57(12):1555–63. https://doi.org/10.1211/jpp.57.12.0005.
49. Hornof M, Toropainen E, Urtti A. Cell culture models of the ocular barriers. Eur J Pharm Biopharm. 2005;60(2):207–25. https://doi.org/10.1016/j.ejpb.2005.01.009.